

Kinetic-theory description of isoscalar dipole modes

V. I. Abrosimov^a, A.Dellafiore^b and F.Matera^b

^a *Institute for Nuclear Research, 03028 Kiev, Ukraine*

^b *Istituto Nazionale di Fisica Nucleare and Dipartimento di Fisica,
Universita' di Firenze, Largo E.Fermi 2, 50125 Firenze, Italy*

Abstract

A semiclassical model, based on a solution of the Vlasov equation for finite systems with moving-surface, is employed to study the isoscalar dipole modes in nuclei. It is shown that, by taking into account the surface degree of freedom, it is possible to obtain an exact treatment of the centre of mass motion. It is also shown that a method often used to subtract the spurious strength in RPA calculations does not always give the correct result. An alternative analytical formula for the intrinsic strength function is derived in a simple confined-Fermi-gas model. In this model the intrinsic isoscalar dipole strength displays essentially a two-resonance structure, hence there are two relevant modes. The interaction between nucleons couples these two modes and changes the compressibility of the system, that we determine by fitting the monopole resonance energy. The evolution of the dipole strength profile is studied as a function of the compressibility of the nuclear fluid. Comparison with recent dipole data shows some qualitative agreement for a soft equation of state, but our model fails to reconcile the monopole and dipole data.

PACS: 24.10.Cn, 24.30.Cz

Keywords: Vlasov equation, isoscalar dipole resonance, nuclear compressibility.

I. INTRODUCTION

The isoscalar dipole mode, excited by the operator

$$O = \sum_i^A r_i^3 Y_{1M}(\hat{\mathbf{r}}_i), \quad (1.1)$$

is particularly interesting because it can give information on the compressibility of nuclear matter [1–3] (Ref. [3] contains a review of experimental and theoretical studies of the isoscalar dipole resonance). This information is complementary to that given by the monopole “breathing” mode [4,5].

From the theoretical point of view the study of the isoscalar dipole mode is complicated by the fact that the operator (1.1) can excite also the centre of mass (c.m.) motion. If the model employed lacks translation invariance, the c.m. excitation may appear as spurious

strength in the calculated response. It is well known that in a perfectly self-consistent random-phase approximation (RPA) the problem of spurious strength does not arise since the c.m. strength is concentrated at zero energy, however, in practice, even a small lack of self-consistency can give substantial spurious dissipation at positive energy (see e.g. [6]).

Recent RPA calculations by two independent groups, using different prescriptions to eliminate the spurious c.m. strength, give somewhat contradictory results [7,8]. The intrinsic isoscalar dipole strength function calculated in Ref. [8] typically shows two main peaks concentrated around 10 – 15 MeV and 20 – 30 MeV. The same feature is not shared by the strength functions calculated in [7], where the low-energy peak has been almost completely eliminated by the subtraction of the spurious strength. More recent calculations performed by other groups [9,10] give results that are in qualitative agreement with those of Ref. [8]. However all RPA calculations start from a zero-order (single-particle) approximation that does not treat the c.m. motion correctly so either perfect self-consistency is required in order to push all the c.m. strength at zero energy, or some procedure must be employed to subtract the spurious strength.

A correct description of the c.m. motion is vital when evaluating the response to the external field (1.1), since that operator excites mainly the c.m. motion. Here we tackle the problem of separating the spurious c.m. excitation from the physically interesting intrinsic excitation by using a semiclassical method based on the Vlasov equation. In Ref. [11], a solution of the linearized Vlasov equation for finite systems with moving surface has been derived, which is well suited to describe c.m. motion (see also Ref. [12]). Clearly quantum calculations are, in principle, more rigorous than a semiclassical one, but our hope is that the physical insight allowed for by the semiclassical method will make our results more transparent.

We calculate the response of nuclei to an external field of the kind

$$V_{ext}(\mathbf{r}, t) = \beta\delta(t)r^3Y_{1M}(\hat{\mathbf{r}}) \quad (1.2)$$

within the model of Ref. [11]. In that model the field (1.2) does not give spurious dissipation at positive energy because, like in a perfectly self-consistent RPA calculation, the c.m. excitation strength is concentrated at zero energy, exactly. Moreover, in the model of [11], contrary to RPA, the c.m. response is treated correctly already in the starting zero-order approximation.

The RPA (including its relativistic generalizations [13–15]) is only one of the two main approaches that have been used to study the dipole compression mode, the other one being the fluid-dynamic approach [2,16]. Our present kinetic-theory approach can be viewed as intermediate between RPA and fluid dynamics.

II. FORMALISM

In this paper we need to evaluate the following kind of response functions:

$$\tilde{\mathcal{R}}_{jk}(\omega) = \frac{1}{\beta} \int d\mathbf{r} r^j Y_{1M}(\hat{\mathbf{r}}) \delta\varrho_k(\mathbf{r}, \omega), \quad (2.1)$$

more specifically, we need the functions $\tilde{\mathcal{R}}_{11}$, $\tilde{\mathcal{R}}_{13}$, $\tilde{\mathcal{R}}_{33}$ (we put a tilde over the moving-surface response functions to distinguish them from the untilded fixed-surface ones). The

fluctuation $\delta\varrho_k(\mathbf{r}, \omega)$ is the time Fourier transform of the density fluctuation $\delta\varrho_k(\mathbf{r}, t)$ induced by an external field $V_{ext}(\mathbf{r}, t) = \beta\delta(t)r^k Y_{1M}(\hat{\mathbf{r}})$. This fluctuation can be obtained by integrating over momentum the phase-space density fluctuation $\delta n_k(\mathbf{r}, \mathbf{p}, t)$ that is given by the solution of the linearized Vlasov equation, either with fixed-surface [17] or with moving-surface [11,12] boundary conditions:

$$\delta\varrho_k(\mathbf{r}, t) = \int d\mathbf{p} \delta n_k(\mathbf{r}, \mathbf{p}, t). \quad (2.2)$$

The solution of the linearized Vlasov equation, both with fixed and moving surface, can be obtained at different levels of approximation.

Here we consider first a zero-order approximation, obtained by neglecting the nucleon-nucleon interaction in the bulk. Note that, while the zero-order approximation of Ref. [17] corresponds to nucleons moving in the static equilibrium mean field and being reflected by the static equilibrium surface, the zero-order approximation of [11] and [12] does take into account partially the density fluctuations induced by the external driving force by considering particle reflections from a moving surface. Thus, what has been called the zero-order approximation in [12] includes more dynamics than the corresponding approximation of [17].

When working with a moving surface it is convenient to introduce a modified density fluctuation $\delta\bar{\varrho}$ that is related to $\delta\varrho$ in the following way. The quantities we are interested in are of the kind (F is an arbitrary function of coordinates)

$$\delta F(t) = \int_{V(t)} d\mathbf{r} F(\mathbf{r}) \varrho(\mathbf{r}, t) - \int_{V_0} d\mathbf{r} F(\mathbf{r}) \varrho_0, \quad (2.3)$$

where ϱ_0 is the equilibrium density, V_0 the equilibrium volume, and $V(t)$ the perturbed time-dependent volume. Consider the integral

$$\int_{V(t)} d\mathbf{r} F(\mathbf{r}) \varrho(\mathbf{r}, t) = \int_{V_0} d\mathbf{r} F(\mathbf{r}) \varrho_0 + \int_{\Delta V(t)} d\mathbf{r} F(\mathbf{r}) \varrho_0 + \int_{V_0} d\mathbf{r} F(\mathbf{r}) \delta\varrho(\mathbf{r}, t) + \mathcal{O}(V_{ext}^2), \quad (2.4)$$

where $\Delta V(t) = V(t) - V_0$; we can include the contribution of $\int_{\Delta V(t)} d\mathbf{r} F(\mathbf{r}) \varrho_0$ into $\int_{V_0} d\mathbf{r} F(\mathbf{r}) \delta\varrho(\mathbf{r}, t)$ if we define [18]

$$\delta\bar{\varrho}(\mathbf{r}, t) = \delta\varrho(\mathbf{r}, t) + \varrho_0 \delta(r - R) \delta R(\hat{\mathbf{r}}, t), \quad (2.5)$$

with $\delta R(\hat{\mathbf{r}}, t)$ giving the fluctuation of the equilibrium radius R induced by the external force. Thus, when evaluating the response functions (2.1) we shall use $\delta\bar{\varrho}$ instead of $\delta\varrho$ and integrate over the equilibrium volume V_0 only.

In the zero-order approximation of [12] the density fluctuation $\delta\varrho(\mathbf{r}, \omega)$ is given by the sum of two terms, one corresponding to the fixed-surface solution of the Vlasov equation, and one giving the moving-surface contribution:

$$\delta\bar{\varrho}^0(\mathbf{r}, \omega) = \delta\bar{\varrho}^0(\mathbf{r}, \omega) + \delta\varrho_{surf}^0(\mathbf{r}, \omega). \quad (2.6)$$

The structure of the last term in this equation is similar to that of the last term in Eq.(2.5) since $\delta\varrho_{surf}^0$ is also proportional to the fluctuation δR of the nuclear surface (cf. Eq. (3.20) of Ref. [12]), so it is convenient to group the two terms together and write

$$\tilde{\mathcal{R}}_{jk}^0(\omega) = \mathcal{R}_{jk}^0(\omega) + \mathcal{S}_{jk}^0(\omega) \quad (2.7)$$

for the response functions in Eq.(2.1).

Here

$$\mathcal{R}_{jk}^0(\omega) = \int dx x^2 \int dy y^2 x^j y^k D_{L=1}^0(x, y, \omega) \quad (2.8)$$

are the zero-order fixed-surface response function calculated according to Ref. [17] (the propagator $D_L^0(x, y, \omega)$ has been defined in [17]), while the quantities

$$\mathcal{S}_{jk}^0(\omega) = \varrho_0 R^{j+2} \delta R_{1M}^0(\omega) + \int d\mathbf{r} r^j Y_{1M}(\hat{\mathbf{r}}) \delta \varrho_{surf}^0(\mathbf{r}, \omega), \quad (2.9)$$

include the contributions both of the last term in Eq.(2.5) and of the surface term $\delta \varrho_{surf}^0$ in Eq.(2.6), the quantity $\delta R_{1M}^0(\omega)$ is given in Eq.(3.21) of Ref. [12]. According to that equation

$$\delta R_{1M}^0(\omega) = -\beta \frac{\chi_k^0(\omega)}{\chi_1(\omega)}. \quad (2.10)$$

The functions $\chi_k^0(\omega)$ and $\chi_1(\omega)$ are given in the Appendix, where the detailed expressions of all the response functions needed in our calculation are also reported.

III. C.M. RESPONSE

Before evaluating the intrinsic excitation strength associated with the external field (1.2), we prove our previous statement that the model of Ref. [11], unlike that of Ref. [17], gives a correct description of c.m. motion already at zero order. From Eq. (A17) we have

$$\tilde{\mathcal{R}}_{11}^0(\omega) = \frac{3}{4\pi} \frac{A}{m\omega^2}, \quad (3.1)$$

as should be expected for a free particle of mass Am (see for example [19]). Since this response function has no poles for $\omega \neq 0$, it does not give spurious dissipation at positive ω .

Another interesting response function is $\tilde{\mathcal{R}}_{13}^0(\omega)$, which, in the present moving-surface model is given by (cf. Eq. (A18))

$$\tilde{\mathcal{R}}_{13}^0(\omega) = R^2 \tilde{\mathcal{R}}_{11}^0(\omega). \quad (3.2)$$

The function $\tilde{\mathcal{R}}_{13}^0(\omega)$ has a direct physical interpretation as the displacement of the nuclear c.m. induced by the external field (1.2):

$$\delta R_{c.m.}^{(3)}(\omega) = \frac{\beta}{A} \tilde{\mathcal{R}}_{13}^0(\omega). \quad (3.3)$$

Van Giai and Sagawa [20] have proposed a method for removing the spurious strength associated with the field $r^3 Y_{1M}(\hat{\mathbf{r}})$. They suggested to use an effective external field of the kind $(r^3 - \eta r) Y_{1M}(\hat{\mathbf{r}})$ and to determine the parameter η by the requirement that the external field does not induce any displacement of the nuclear c.m.:

$$\delta R_{c.m.}^{(eff)}(\omega) = 0. \quad (3.4)$$

By using this prescription in a fluid-dynamic model, they determined $\eta = \frac{5}{3} \langle r^2 \rangle$, where $\langle r^2 \rangle$ is the nucleus mean square radius (in our model $\langle r^2 \rangle = \frac{3}{5}R^2$). Here we do not need to use the effective field $(r^3 - \eta r)$ because the moving-surface model employed does not give any spurious dissipation, however, if we do this, we find

$$\delta R_{c.m.}^{(eff)}(\omega) = \frac{\beta}{A} [\tilde{\mathcal{R}}_{13}^0(\omega) - \eta \tilde{\mathcal{R}}_{11}^0(\omega)], \quad (3.5)$$

giving

$$\eta = \frac{\tilde{\mathcal{R}}_{13}^0(\omega)}{\tilde{\mathcal{R}}_{11}^0(\omega)}. \quad (3.6)$$

Using Eq.(3.2) we get $\eta = R^2$, in agreement with [20]. However we note that this simple result is obtained in a model that already has the correct translation-invariance property and that this procedure with $\eta = R^2$ cannot be used as a general prescription for subtracting the spurious strength in non-translationally-invariant models. Had we used this prescription within the fixed-surface model of Ref [17], that can be taken as an example of a case in which the problem of spurious dissipation appears, we would have found

$$\eta = \frac{\mathcal{R}_{13}^0(\omega)}{\mathcal{R}_{11}^0(\omega)}, \quad (3.7)$$

but now the two response functions in the numerator and denominator are no longer proportional (cf. Eq.(A2)), and we would need a complex and ω -dependent parameter η to subtract the spurious strength.

In order to allow for a more quantitative appreciation of spurious effects, in Fig.1 we show the zero-order response function calculated in the fixed-surface approximation of Eq.(A2), that is with no corrections for c.m. effects (dotted curve), and the same response function calculated for the effective operator $(r^3 - R^2 r)$ (dashed curve). This effective operator drastically reduces the response (by almost 90% for $A = 208$), but it leaves the intrinsic strength at the same energy of the uncorrected response. The solid curve in Fig.1 instead shows the result of our present moving-surface model, to be discussed more extensively in the next section. The quantities plotted in this and in the two following figures are the strength functions $S(\hbar\omega)$, related to the respective response functions by $S(\hbar\omega) = -\frac{1}{\pi} \text{Im} \mathcal{R}(\hbar\omega)$. In the translation-invariant model the strength function includes a δ -function at the origin, which is not shown. The excitation energy is $E = \hbar\omega$.

IV. INTRINSIC DIPOLE STRENGTH

A. Confined Fermi gas

After having shown that the model of Ref. [11] does not introduce any spurious dissipation at $\omega \neq 0$, we are now in a position to evaluate the nuclear response to the external field (1.2), without having to worry about spurious effects. The response function $\tilde{\mathcal{R}}_{33}^0$ is given

by Eq.(A19). This response function is qualitatively different from those discussed in the previous section. Like $\tilde{\mathcal{R}}_{11}^0$ and $\tilde{\mathcal{R}}_{13}^0$, it does contain a part that is proportional to $\frac{1}{\omega^2}$ (given by Eq. (A20)) and represents c.m. excitation. This part does not give any strength at $\omega \neq 0$. In addition to the c.m. response, $\tilde{\mathcal{R}}_{33}^0$ contains also an intrinsic part given by Eq.(A21). In terms of the variable ω the intrinsic response function (A21) reads

$$\tilde{\mathcal{R}}_{intr}^0(\omega) = \mathcal{R}_{33}^0(\omega) - \frac{3A}{4\pi} \frac{R^4}{m} \frac{1}{\omega^2} \left\{ 1 - \frac{\left[1 - \frac{1}{2} \omega^2 \frac{\mathcal{R}_{13}^0(\omega)}{m_{13}^1} \right]^2}{1 - \frac{1}{2} \omega^2 \frac{\mathcal{R}_{11}^0(\omega)}{m_{11}^1}} \right\}, \quad (4.1)$$

with the ω -moments m_{jk}^p related to the s -moments (A22) by

$$m_{jk}^p = \left(\frac{v_F}{R} \right)^{p+1} \mathcal{M}_{jk}^p. \quad (4.2)$$

Equation (4.1) does express the intrinsic response function associated with the operator (1.1) in terms of response functions calculated in the underlying non-translationally-invariant model, the analogous expression given by the widely used prescription $r^3 \rightarrow (r^3 - \eta r)$ (with real η) is

$$\mathcal{R}_{eff}^0(\omega) = \mathcal{R}_{33}^0(\omega) - 2\eta \mathcal{R}_{13}^0(\omega) + \eta^2 \mathcal{R}_{11}^0(\omega). \quad (4.3)$$

We can easily check that, if we were allowed to make the approximation $\mathcal{R}_{13}^0(\omega) = R^2 \mathcal{R}_{11}^0(\omega)$, which is not valid in the fixed-surface model, then Eq. (4.1) would be equivalent to Eq. (4.3), but the two formulae are different in general. The intrinsic strength function associated with the response function (4.1) is shown by the solid curves in Figs. 1 and 2, while that given by Eq.(4.3) with $\eta = R^2$ is given by the dashed curves in the same figures. The strength distributions given by the two formulae (4.1) and (4.3) are qualitatively different, in spite of the fact that they give the same moments m^1 and m^{-1} . Actually, using the high-frequency expansion [21]

$$\mathcal{R}_{jk}^0(\omega)|_{\omega \rightarrow \infty} = \frac{2m_{jk}^1}{\omega^2} + \mathcal{O}\left(\frac{1}{\omega^3}\right), \quad (4.4)$$

Eq. (4.1) gives

$$\int_0^\infty d(\hbar\omega) \hbar\omega \left[-\frac{1}{\pi} \text{Im} \tilde{\mathcal{R}}_{intr}^0(\omega) \right] = \frac{3\hbar^2}{14\pi m} AR^4 \quad (4.5)$$

for the intrinsic energy-weighted sum rule \tilde{m}_{intr}^1 associated with the operator (1.1), in agreement with Eq. (A.4) of Ref. [20] (in our model $\langle r^4 \rangle = \frac{3}{7} R^4$).

The m^{-1} moment is also the same for the two response functions (4.1) and (4.3). Taking the limit of small frequency, we get

$$\lim_{\omega \rightarrow 0} \tilde{\mathcal{R}}_{intr}^0(\omega) = \lim_{\omega \rightarrow 0} \mathcal{R}_{eff}^0(\omega) = -\frac{6}{35\pi} \frac{AR^6}{K_{FG}}, \quad (4.6)$$

where $K_{FG} = 6\epsilon_F$ is the Fermi-gas incompressibility parameter. This limit is related to the hydrodynamic sum rule

$$\tilde{m}_{intr}^{-1} = \int_0^\infty d\omega \frac{1}{\omega} \left[-\frac{1}{\pi} \text{Im} \tilde{\mathcal{R}}_{intr}^0(\omega) \right] \quad (4.7)$$

by [21]

$$\lim_{\omega \rightarrow 0} \tilde{\mathcal{R}}_{intr}^0(\omega) = -2\tilde{m}_{intr}^{-1}. \quad (4.8)$$

Having established the value of the two moments \tilde{m}_{intr}^1 and \tilde{m}_{intr}^{-1} , we can calculate the mean excitation energy as

$$\begin{aligned} \hbar\tilde{\omega}_{1-1} &= \sqrt{\frac{\tilde{m}_{intr}^1}{\tilde{m}_{intr}^{-1}}} \\ &= \hbar \sqrt{\frac{3}{2} \frac{K_{FG}}{m \langle r^2 \rangle}}, \end{aligned} \quad (4.9)$$

in agreement with [2], where a phenomenological incompressibility parameter K was used instead of K_{FG} . Since $K_{FG} \approx 200$ MeV (for $R = 1.2 A^{1/3}$ fm), while the phenomenological value used in [2] was $K = 220$ MeV, we see that, already at the Fermi-gas level, we have a reasonable estimate for the mean excitation energy of the isoscalar dipole strength. What is unrealistic in the Fermi gas model, is the pressure P exerted by the nuclear fluid, but the incompressibility, defined as $K \equiv 9 \frac{\partial P}{\partial \rho}$, happens to be within the range of 210 ± 30 MeV compatible with the monopole data [4]. In any case we can always change the compressibility of the system by switching on the residual interaction between nucleons.

B. Changing the compressibility

So far we have treated the nucleus like a gas of non-interacting fermions confined to a spherical cavity with perfectly reflecting walls that are allowed to move under the action of the gas pressure induced by the external field, taking into account the interaction between nucleons changes the compressibility of this nuclear fluid.

Rather than embarking in numerical calculations, here we give only a simple estimate of the main effects that are expected when the nucleon-nucleon interaction is switched on and, in order to keep the analytic insight allowed for by our semiclassical approach, we assume a very schematic, separable, effective interaction of the dipole-dipole type:

$$u(\mathbf{r}, \mathbf{r}') = \alpha \sum_M r r' Y_{1M}(\hat{\mathbf{r}}) Y_{1M}^*(\hat{\mathbf{r}}'). \quad (4.10)$$

The parameter \mathcal{F}_0 , determining the strength of the interaction, will be related to the compressibility, which is the relevant parameter in this context. Then the fixed-surface collective response functions $\mathcal{R}_{1k}(\omega)$, given by the solution of the RPA-type integral equation (5.28) of Ref. [17] are:

$$\mathcal{R}_{1k}(\omega) = \frac{\mathcal{R}_{1k}^0(\omega)}{1 - \alpha \mathcal{R}_{11}^0(\omega)} \quad (k = 1, 3), \quad (4.11)$$

and

$$\mathcal{R}_{33}(\omega) = \mathcal{R}_{33}^0(\omega) + \alpha \frac{[\mathcal{R}_{13}^0(\omega)]^2}{1 - \alpha \mathcal{R}_{11}^0(\omega)}. \quad (4.12)$$

Now, if we replace the Fermi gas fixed-surface response functions $\mathcal{R}_{jk}^0(\omega)$ with the above collective response functions $\mathcal{R}_{jk}(\omega)$ in Eq.(4.1), we obtain a new intrinsic response function

$$\begin{aligned} \tilde{\mathcal{R}}_{intr}(\omega) = & \mathcal{R}_{33}^0(\omega) + \alpha \frac{[\mathcal{R}_{13}^0(\omega)]^2}{1 - \alpha \mathcal{R}_{11}^0(\omega)} \\ & - \frac{3A R^4}{4\pi m \omega^2} \left\{ 1 - \frac{\left[1 - \frac{1}{2} \omega^2 \frac{\mathcal{R}_{13}^0(\omega)}{m_{13}^1} \frac{1}{1 - \alpha \mathcal{R}_{11}^0(\omega)} \right]^2}{1 - \frac{1}{2} \omega^2 \frac{\mathcal{R}_{11}^0(\omega)}{m_{11}^1} \frac{1}{1 - \alpha \mathcal{R}_{11}^0(\omega)}} \right\}. \end{aligned} \quad (4.13)$$

The energy-weighted moment \tilde{m}_{intr}^1 of this response function is still given by Eq.(4.5), as can be easily checked by studying the large- ω limit. Thus we are confident that, even if the dipole-dipole residual interaction (4.10) violates translation invariance, we are not introducing any spurious strength in our intrinsic response function (4.13).

Contrary to the first moment m^1 , the inverse moment m^{-1} is altered by the residual interaction. This can be checked by evaluating the limit

$$\lim_{\omega \rightarrow 0} \tilde{\mathcal{R}}_{intr}(\omega) = -\frac{6}{35\pi} \frac{AR^6}{6\epsilon_F [1 - \alpha \mathcal{R}_{11}^0(0)]} \left[1 - \frac{5}{14} \alpha \mathcal{R}_{11}^0(0) \right], \quad (4.14)$$

where

$$\mathcal{R}_{11}^0(0) = -\frac{2}{5} \frac{9A R^2}{16\pi \epsilon_F}. \quad (4.15)$$

Equation (4.14) can be written as

$$\lim_{\omega \rightarrow 0} \tilde{\mathcal{R}}_{intr}(\omega) = -\frac{6}{35\pi} \frac{AR^6}{K}, \quad (4.16)$$

with

$$K = 6\epsilon_F \frac{1 - \alpha \mathcal{R}_{11}^0(0)}{1 - \frac{5}{14} \alpha \mathcal{R}_{11}^0(0)}. \quad (4.17)$$

By following exactly the same procedure for monopole vibrations, for which we assume a monopole residual interaction of the kind

$$u(r, r') = \frac{\beta}{4\pi} r^2 r'^2, \quad (4.18)$$

we find an analogous expression for the monopole incompressibility:

$$K_{mon} = 6\epsilon_F \frac{1 - \beta \mathcal{R}_{L=0}^0(0)}{1 - \frac{21}{26} \beta \mathcal{R}_{L=0}^0(0)}, \quad (4.19)$$

where $\mathcal{R}_{L=0}^0(0)$ is the zero-frequency limit of the monopole response function, analogous to (4.15). We can determine K_{mon} by comparison with the data on giant monopole resonances (see Table I) and then, by assuming $K = K_{mon}$, we can study the dipole response.

In our simplified scheme for taking into account the residual interaction between nucleons, we replace the Fermi-gas intrinsic response function (4.1) with Eq. (4.13). Thus Eq.(4.13) becomes our final expression for the intrinsic isoscalar dipole response function, it is a generalization of the confined-Fermi-gas expression (4.1) to a confined fluid of interacting nucleons with incompressibility K . At first we treat K as a free parameter and study its effect on the dipole response function, then we determine the value of K by comparison with the monopole-resonance data and use this value to compare with the dipole-resonance data.

The strength function associated with the response function (4.13) is shown in Fig. 3 for three values of the incompressibility ($K = K_{FG}$, $K < K_{FG}$, and $K > K_{FG}$). When the system becomes softer, part of the strength shifts from the high-energy peak towards the low-energy peak, at about 13 MeV in Lead. The position of the two centroids is also slightly changed, but the main effect is the change in the relative weight of the two peaks. This behavior is similar to that found in the relativistic approach of Ref. [13], the position of the peaks is also similar for comparable values of K . However, unlike Ref. [13], we do not see any qualitative difference in the sensitivity of the two peaks to the compressibility of the system.

We finally note that for $K > K_{FG}$ the strength moves to higher energy.

C. Comparison with data

In Table I we report experimental centroid energies of the giant monopole resonance taken from Ref. [22], together with our calculated values. A reasonable agreement with experiment is obtained for $K_{mon} = 180$ MeV.

In Fig.4 we compare our energy-weighted strength functions with the recent data of Ref. [23] for ^{208}Pb , ^{116}Sn and ^{90}Zr . The quantity plotted in the figure is

$$y(E) = 100E \left(-\frac{1}{\pi} \text{Im} \tilde{\mathcal{R}}_{intr}(E) \right) / \tilde{m}_{intr}^1, \quad (4.20)$$

where $E = \hbar\omega$ is the excitation energy. The solid curve shows our confined-Fermi-gas response, that is the energy-weighted isoscalar dipole strength for an assembly of non-interacting nucleons with incompressibility $K \approx 200$ MeV. Our strength integrated up to $\hbar\omega = 40$ MeV exhausts about 90% of the energy-weighted sum rule \tilde{m}_{intr}^1 , while integrating up to 100 MeV exhausts about 99% of the energy-weighted sum rule. It is important to note that the data overshoot this sum rule [23]. The reasons for this overshooting are not clear to us, since, unlike the isovector dipole, no enhancement factor of the energy-weighted sum rule is expected in this case [21].

The experimental finding of [23] that the isoscalar dipole strength consists of two components is qualitatively reproduced by our semiclassical model (at the Fermi gas level the two resonances correspond to two complex zeroes of the function $\chi_1(s)$ of Eq.(A13) [12]). In this respect our results are also in qualitative agreement with the quantal RPA calculations of [8–10] and [13–15], that predict a two-resonance structure in the isoscalar dipole response.

For the confined Fermi gas (solid line) the position of the two peaks is too high in energy. Taking into account the residual interaction (dashed line) improves the agreement with data, but does not completely remove the discrepancy, especially for the high-energy peak.

The dashed curve in Fig.4 has been calculated for $K = 180$ MeV, which has been determined by fitting the energy of the isoscalar monopole resonance within the same model.

Our value of K lies at the lower end of the uncertainty range indicated in Ref. [4] and is somewhat smaller than the values reported in Ref. [5]. However these values refer to saturated and symmetric ($N = Z$) nuclear matter. The small discrepancy is probably due to the fact that we are using a sharp-surface model, while of course experiments are performed on real nuclei that have a diffuse surface, thus our value of K does not refer to the density in the interior of nuclei, but rather to some average density that takes into account surface diffuseness. Also, in real nuclei N is larger than Z and, as pointed out in [24], K decreases with increasing asymmetry.

By comparing the two curves shown in Fig.4, we can say that an attractive interaction between nucleons, that decreases the value of K with respect to the initial value of 200 MeV, improves the agreement with data, but the position of the high-energy peak remains too high in energy, even for the rather small value $K = 180$ MeV, suggested by our fit to monopole data. Further decrease of K would shift the response towards lower energy and would redistribute the strength by enhancing the low-energy peak and depleting the high-energy one, moreover this would give too small values for the monopole-resonance centroid energies. The coupling of the two resonances in the isoscalar dipole response due to the residual interaction is a novel effect displayed by our calculation and, although the position of the peaks is not much affected by the compressibility, we find that the strength associated with them is quite sensitive to the value of K .

Another qualitative feature of the data that is well reproduced by our calculations is the $A^{-\frac{1}{3}}$ dependence of the peak positions [23]. Actually, an interesting property of the response function (4.13) is that, if K/ϵ_F is independent of A , then this quantity, like the functions \mathcal{R}_{jk}^0 , can be expressed in terms of a universal function of the dimensionless parameter s defined in the Appendix:

$$\tilde{\mathcal{R}}_{intr.}(s) = \mathcal{N}_{33}(A)u(s). \quad (4.21)$$

The function $u(s)$ is the same for all spherical nuclei and its explicit expression can be easily derived from the equations given in the Appendix. The mass number A of the particular nucleus being studied enters only through the normalization factor

$$\mathcal{N}_{33}(A) = \frac{9A}{16\pi} \frac{R^6}{\epsilon_F} \quad (4.22)$$

and does not affect the position of the resonances in the variable s . Since $s \propto A^{\frac{1}{3}}$, the scaling property (4.21) of the response function (4.13) results in an $A^{-\frac{1}{3}}$ dependence of the peak positions in excitation energy.

In conclusion, our model is able to reproduce some of the features displayed by the data like the two-resonance structure of the response and the A -dependence of the peak position, but, even after an accurate subtraction of the spurious c.m. strength for which a new formula has been derived, it fails to reconcile the monopole and dipole data. This failure is shared by our semiclassical model with the quantal RPA calculations of Ref.s [7–10] and [13–15].

V. ACKNOWLEDGEMENTS

V.I.A. has been partially supported by INFN and MURST, Italy. A.D. is grateful for the warm hospitality extended to him during his visit to the Institute for Nuclear Research, Kiev.

APPENDIX: RESPONSE FUNCTIONS

In this Appendix we give explicit expressions for the functions $\tilde{\mathcal{R}}_{11}^0$, $\tilde{\mathcal{R}}_{13}^0$ and $\tilde{\mathcal{R}}_{33}^0$. Instead of the variable ω , it is convenient to use the dimensionless variable

$$s = \frac{\omega}{v_F/R}, \quad (\text{A1})$$

where v_F is the Fermi velocity, we shall use also the Fermi energy ϵ_F to characterise our systems. Moreover we add a vanishingly small positive imaginary part to the variable s in order to define the behaviour of the response functions at poles: $s \rightarrow s + i\varepsilon$.

The fixed-surface part of the response functions (2.7) can be calculated by using the propagator $D_{L=1}^0(r, r', \omega)$ given in Ref. [17]. The explicit expression for A non-interacting nucleons at zero temperature contained in a spherical cavity of radius R is:

$$\mathcal{R}_{jk}^0(s) = \frac{9A}{16\pi} \frac{1}{\epsilon_F} \sum_{n=-\infty}^{+\infty} \sum_{N=\pm 1} \int_0^1 dx x^2 s_{nN}(x) \frac{Q_{nN}^{j*}(x) Q_{nN}^k(x)}{s - s_{nN}(x)}. \quad (\text{A2})$$

We have defined

$$s_{nN}(x) = \frac{n\pi + N\alpha(x)}{x}, \quad (\text{A3})$$

and $\alpha(x) = \arcsin(x)$, while the Fourier coefficients $Q_{nN}^k(x)$ are defined according to Ref. [17], they are the classical limit of the radial matrix elements of the operator r^k . The coefficients needed in our calculations are:

$$Q_{nN}^1(x) = (-)^n R \frac{1}{s_{nN}^2(x)} \quad (\text{A4})$$

and

$$Q_{nN}^3(x) = (-)^n R^3 \frac{3}{s_{nN}^2(x)} \left(1 + \frac{4}{3} N \frac{\sqrt{1-x^2}}{s_{nN}(x)} - \frac{2}{s_{nN}^2(x)} \right). \quad (\text{A5})$$

The functions $\chi_k^0(s)$ and $\chi_1(s)$, associated with the moving-surface part of the response (cf. Eq. (2.10)), are given by

$$\chi_k^0(s) = \frac{9A}{8\pi} \frac{1}{R^3} \sum_{n=-\infty}^{+\infty} \sum_{N=\pm 1} \int_0^1 dx x^2 s_{nN}(x) \frac{(-)^n Q_{nN}^k(x)}{s - s_{nN}(x)}, \quad (\text{A6})$$

and

$$\chi_1(s) = -\frac{9A}{4\pi} \epsilon_F s \sum_{n=-\infty}^{+\infty} \sum_{N=\pm 1} \int_0^1 dx x^2 \frac{1}{s - s_{nN}(x)}. \quad (\text{A7})$$

The function $\chi_1(s)$ is the $L = 1$ component of $\chi_L(s)$, defined in Eq.(3.23) of [12], we have used the pole expansion of the cotangent to write it in the present form, while the functions $\chi_k^0(s)$ give the numerator of Eq. (3.21) of the same reference for external fields $r^k Y_{1M}(\hat{\mathbf{r}})$. We notice the similarity between the fixed-surface response function (A2) and

the two functions $\chi_k^0(s)$ and $\chi_1(s)$ appearing in the moving-surface part of the response, in particular the integrand in all these functions has the same poles, while the numerators are different.

By using the explicit expressions of the Fourier coefficients (A4) and (A5) and, repeatedly, the identity

$$\frac{1}{s_{nN}} \frac{1}{s - s_{nN}} = \frac{1}{s} \left(\frac{1}{s_{nN}} + \frac{1}{s - s_{nN}} \right) \quad (\text{A8})$$

it is possible to express the fixed-surface response functions in terms of the functions $\chi_k^0(s)$ and $\chi_1(s)$. A useful identity, obtained in this way, is

$$\frac{2\epsilon_F}{R^4} \mathcal{R}_{1k}^0(s) = \frac{1}{s^2} (\chi_k^0(s) - \chi_k^0(0)) \quad (k = 1, 3). \quad (\text{A9})$$

We do not report here the analogous expression for $\mathcal{R}_{33}^0(s)$ since it is too involved. Moreover

$$\chi_1^0(s) = -\frac{1}{2\epsilon_F R^2} \frac{\chi_1(s)}{s^2}, \quad (\text{A10})$$

$$\chi_3^0(s) = -\frac{3}{2\epsilon_F} \frac{\chi_1(s)}{s^2} \left(1 - \frac{2}{s^2}\right) - \frac{3A}{\pi} \frac{1}{s^2} \left[1 - \frac{3}{4} \int_0^1 dx x^2 \sum_{N=\pm 1} \frac{\sin(sx + N\alpha(x))}{\sin(sx - N\alpha(x))}\right], \quad (\text{A11})$$

and

$$\chi_3^0(0) = R^2 \chi_1^0(0) = -\frac{3A}{4\pi}. \quad (\text{A12})$$

The advantage of expressing the fixed-surface response functions and the functions $\chi_k^0(s)$ in terms of the function $\chi_1(s)$ is due to the fact that the infinite sum over n in $\chi_1(s)$ can be performed exactly, consequently we can obtain exact closed expressions for all these functions within this model. A useful closed expression for $\chi_1(s)$ is

$$\chi_1(s) = -3\epsilon_F \frac{3A}{4\pi} s \int_0^1 dx x^3 \frac{\sin(2sx)}{\sin^2(sx) - x^2}. \quad (\text{A13})$$

Thus, by using the relations given above, we can connect the zero-order fixed-surface and moving-surface solutions of the Vlasov equation obtained in Refs. [11,17]. This is particularly simple for \mathcal{S}_{11}^0 and \mathcal{S}_{13}^0 since

$$\mathcal{S}_{1k}^0(s) = -\frac{R^4}{2\epsilon_F} \frac{\chi_k^0(s)}{s^2} \quad (k = 1, 3), \quad (\text{A14})$$

while it is somewhat more complicated for \mathcal{S}_{33}^0 since

$$\mathcal{S}_{33}^0(s) = -\frac{R^4}{2\epsilon_F} \frac{\chi_3^0(s)}{s^2} \frac{\chi_3^0(s)}{\chi_1(s)}. \quad (\text{A15})$$

By inserting $\chi_k^0(s)$ obtained from Eq. (A9) into (A14), we get

$$\mathcal{S}_{1k}^0(s) = -\mathcal{R}_{1k}^0(s) + \frac{3A R^{k+1}}{4\pi} \frac{1}{2\epsilon_F s^2} \quad (k = 1, 3), \quad (\text{A16})$$

that gives

$$\tilde{\mathcal{R}}_{11}^0(s) = \frac{3A R^2}{4\pi} \frac{1}{2\epsilon_F s^2} \quad (\text{A17})$$

and

$$\tilde{\mathcal{R}}_{13}^0(s) = R^2 \tilde{\mathcal{R}}_{11}^0(s) \quad (\text{A18})$$

for two of the full response functions in (2.7).

For $\tilde{\mathcal{R}}_{33}^0$, we obtain

$$\tilde{\mathcal{R}}_{33}^0(s) = \tilde{\mathcal{R}}_{c.m.}^0(s) + \tilde{\mathcal{R}}_{intr}^0(s), \quad (\text{A19})$$

with

$$\tilde{\mathcal{R}}_{c.m.}^0(s) = \frac{3A R^6}{4\pi} \frac{1}{2\epsilon_F s^2} \quad (\text{A20})$$

and

$$\tilde{\mathcal{R}}_{intr}^0(s) = \mathcal{R}_{33}^0(s) - \frac{3A R^6}{4\pi} \frac{1}{2\epsilon_F s^2} \left\{ 1 - \frac{\left[1 - \frac{1}{2} s^2 \frac{\mathcal{R}_{13}^0(s)}{\mathcal{M}_{13}^1} \right]^2}{1 - \frac{1}{2} s^2 \frac{\mathcal{R}_{11}^0(s)}{\mathcal{M}_{11}^1}} \right\} \quad (\text{A21})$$

giving the c.m. and intrinsic response, respectively. The last equation expresses the intrinsic response function for the operator (1.1) in terms of non-translationally-invariant response functions and is the main result of the present paper. It is an exact relation within the present model (confined Fermi gas). The moments

$$\mathcal{M}_{jk}^p = \int_0^\infty ds s^p \left[-\frac{1}{\pi} \text{Im} \mathcal{R}_{jk}^0(s) \right] \quad (\text{A22})$$

are defined in terms of the fixed-surface response functions and they can be easily evaluated from (A2). Explicitly: $\mathcal{M}_{11}^1 = \frac{1}{3} \frac{9A R^2}{16\pi \epsilon_F}$, $\mathcal{M}_{13}^1 = R^2 \mathcal{M}_{11}^1$, and $\mathcal{M}_{33}^1 = \frac{11}{7} R^4 \mathcal{M}_{11}^1$.

An essential property of the intrinsic response function (A21) is that its limit for $s \rightarrow 0$ is finite.

REFERENCES

- [1] M.N.Harakeh, Phys. Lett. 90B (1980) 13
- [2] S.Stringari, Phys. Lett. 108B (1982) 232
- [3] U.Garg, RIKEN Review 23 (1999) 65
- [4] J.P.Blaizot, Phys. Rep. 64 (1980) 171
- [5] J.P.Blaizot, J.F.Berger, J.Dechargé and M.Girod, Nucl. Phys. A591 (1995) 435
- [6] F.Catara, E.G.Lanza, M.A.Nagarajan, and A.Vitturi, Nucl. Phys. A624 (1997) 449
- [7] I.Hamamoto, H.Sagawa and X.Z.Zhang, Phys. Rev. C 57 (1998) R1064
- [8] G.Colò, N.Van Giai, P.F.Bortignon and M.R.Quaglia, Phys. Lett. B 485 (2000) 362
- [9] S.Shlomo and A.I.Sanzhur, arXiv:nucl-th/0011098
- [10] M.L.Gorelik and M.H.Urin, arXiv:nucl-th/0104001
- [11] V. Abrosimov, M. Di Toro and V. Strutinsky, Nucl. Phys. A562 (1993) 41
- [12] V. Abrosimov, A.Dellafiore and F. Matera, Nucl. Phys. A653 (1999) 115
- [13] D.Vretenar, A.Wandelt and P.Ring, Phys. Lett. B 487 (2000) 334
- [14] J. Piekarewicz, Phys. Rev. C 62 (2000) 051304(R)
- [15] J. Piekarewicz, arXiv:nucl-th/0103016
- [16] V.M.Kolomietz and S.Shlomo, Phys Rev. C 61 (2000) 064302
- [17] D.M.Brink, A.Dellafiore and M.Di Toro, Nucl. Phys A456 (1986) 205
- [18] B.K.Jennings and A.D.Jackson, Phys. Rep. 66 (1980) 141
- [19] P.C.Martin, Many-Body Physics, ed. C.De Witt and R. Balian (Gordon and Breach, N.Y., 1968)
- [20] Nguyen Van Giai and H. Sagawa, Nucl. Phys. A371 (1981) 1
- [21] E. Lipparini and S. Stringari, Phys. Rep. 175 (1989) 103
- [22] D.H. Youngblood, H.L. Clark and Y.-W.Lui, Phys. Rev. Lett. 82 (1999) 691
- [23] H.L.Clark, Y.-W.Lui, and D.H. Youngblood, Phys. Rev. C 63 (2001) 031301
- [24] S. Yoshida, H. Sagawa, and N. Takigawa, Phys. Rev. C 58 (1998) 2796

TABLES

TABLE I. Experimental and calculated energies of giant monopole resonance. Data from Ref. [22]

Nucleus	Exp. energy	Calc. energy
	MeV	MeV
^{208}Pb	14.17 ± 0.28	14.1
^{116}Sn	16.07 ± 0.12	17.2
^{90}Zr	17.89 ± 0.20	18.7

FIGURE CAPTIONS

Fig.1 Isoscalar dipole response in fixed- and moving-surface models. The dotted line shows the fixed-surface response for radial dependence of operator $Q(r) = r^3$, while the dashed line is for the effective operator $Q(r) = r^3 - R^2r$. The solid line shows the zero-order moving-surface strength given by Eq.(4.1).

Fig.2 The dashed and solid curves are the same as in Fig.1 . Note the change of vertical scale.

Fig.3 Dipole strength for different value of incompressibility parameter. The solid curve shows our Fermi-gas result.

Fig.4 Comparison of our energy-weighted strength functions with experimental data of Ref. [23] for ^{208}Pb (a), ^{116}Sn (b) and ^{90}Zr (c). The solid curve shows the Fermi-gas result, corresponding to incompressibility $K \approx 200$ MeV, the dashed curve is for interacting nucleons with $K = 180$ MeV.

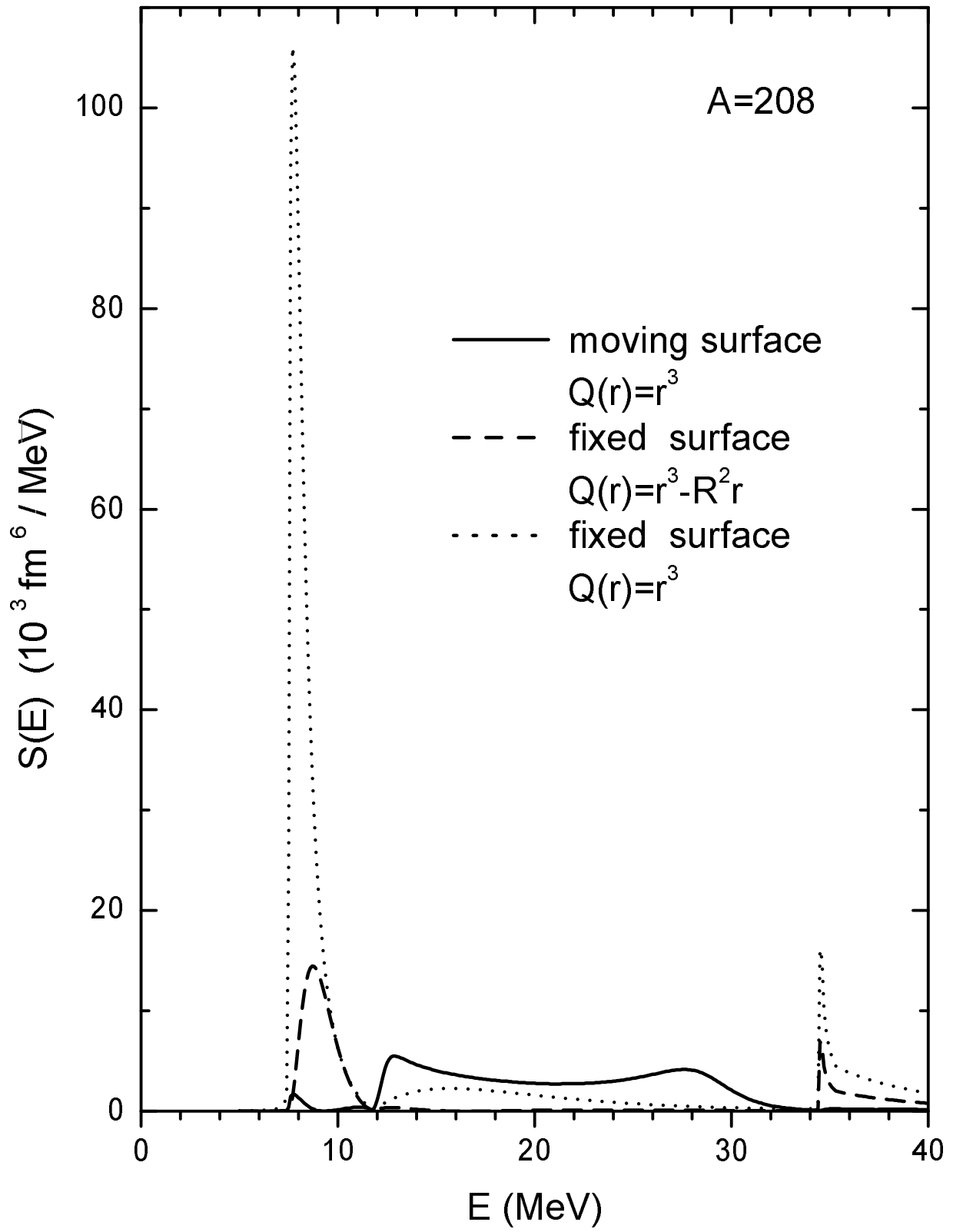


Fig. 1

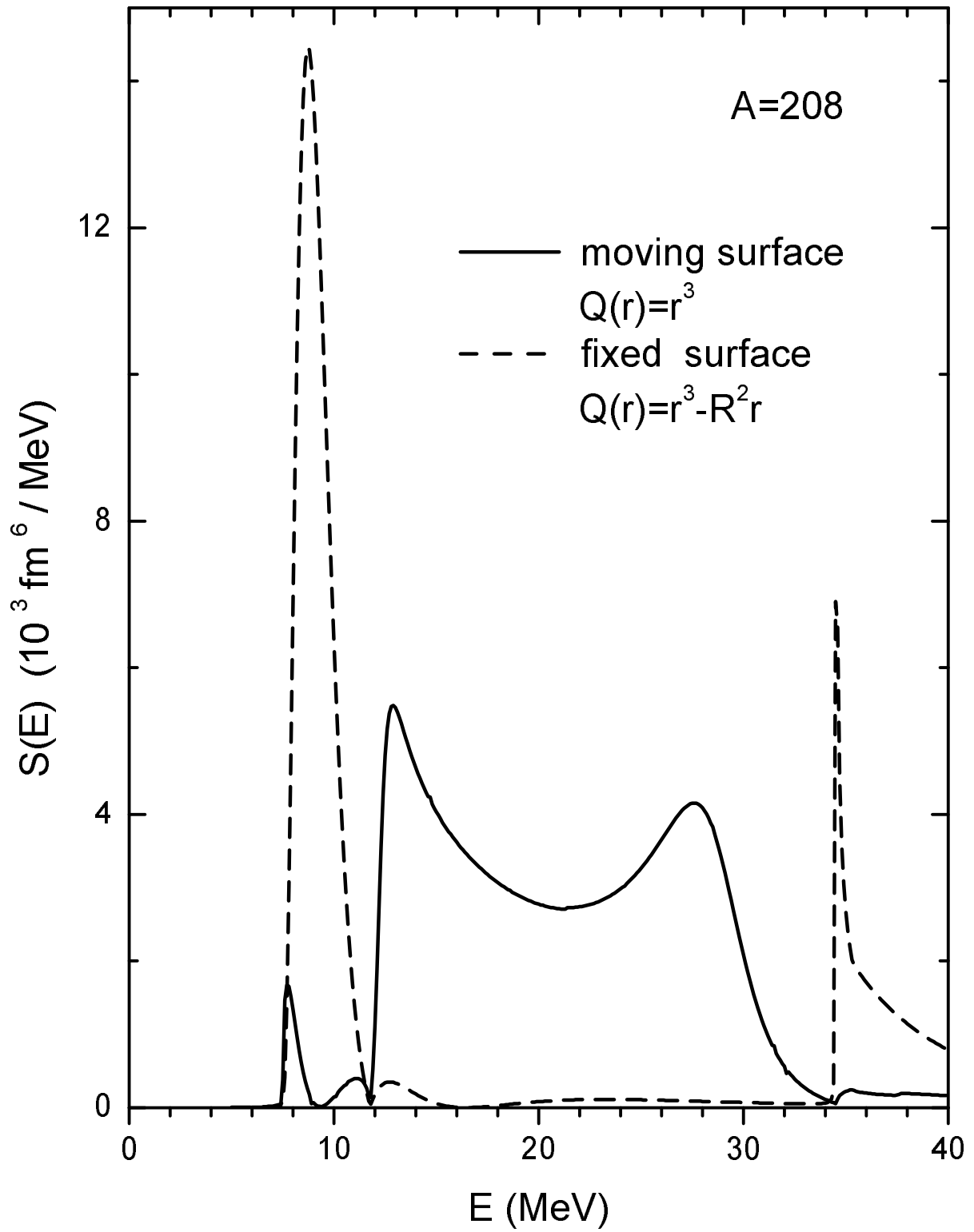


Fig. 2

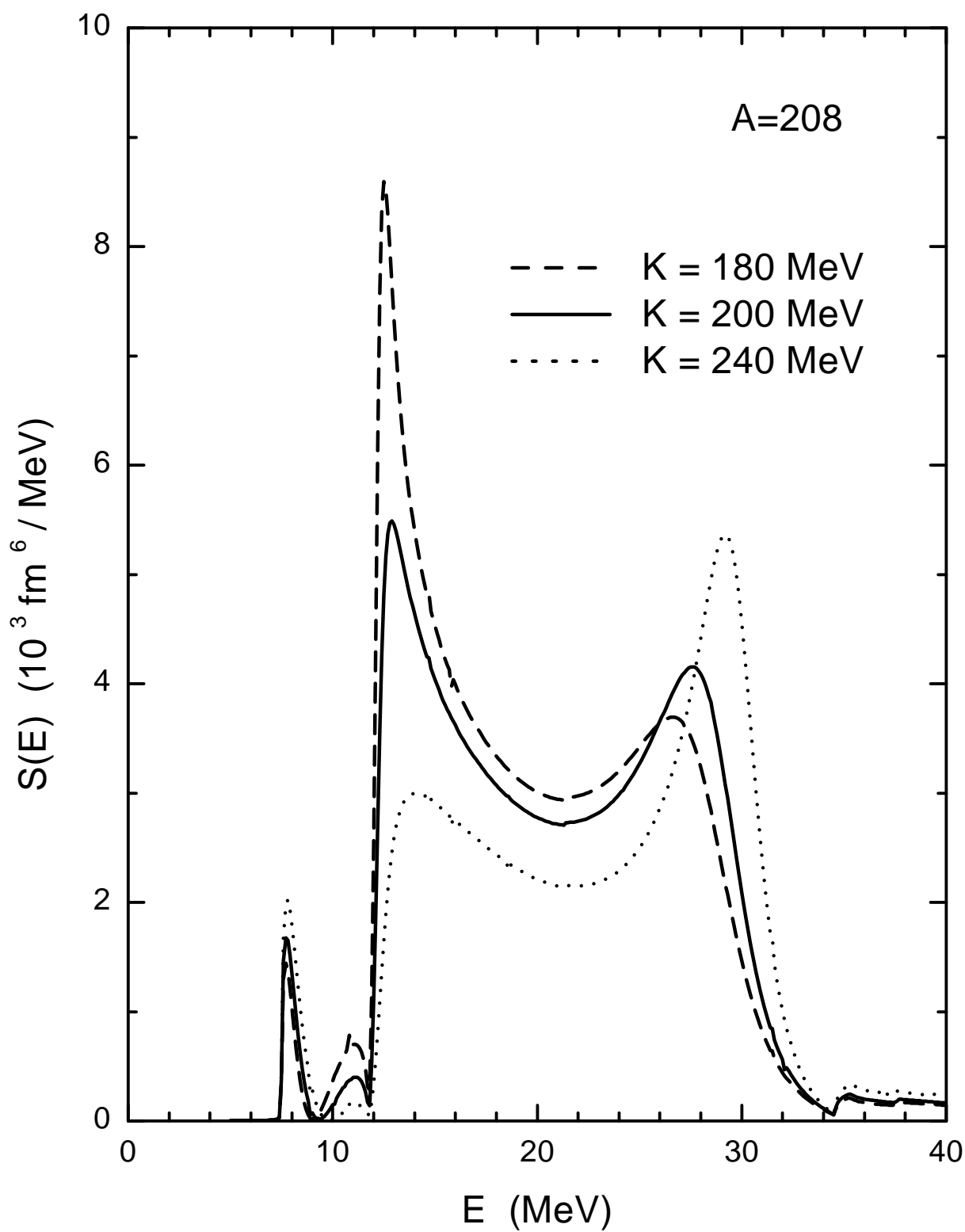


Fig. 3

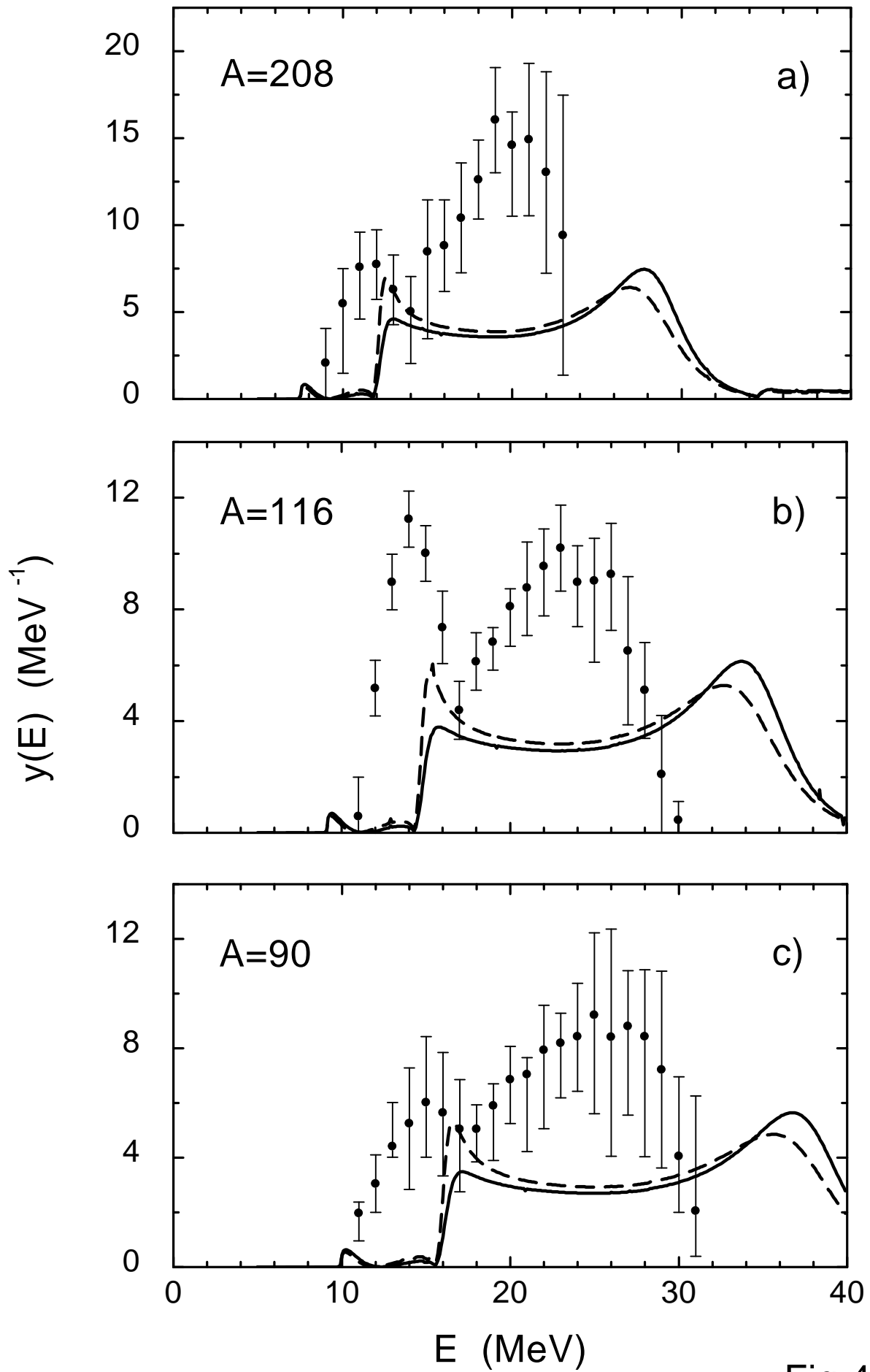


Fig.4